Excitation of alkali-metal-like ions by electron impact

P. A. Hervieux and C. Guet
Département de Recherche Fondamentale Matière Condensée, LI2A, Centre d' Etudes Nucléaires de Grenoble, 85X, 38041 Grenoble CEDEX, France
(Received 9 September 1992)

Differential and total cross sections for the dipole excitation of valence electrons in alkali-metal-like ions by electron impact well above the threshold energy are calculated in the generalized Born approximation and in a semiclassical approximation. The angular distribution is peaked at an angle which is essentially defined by energy-momentum-matching conditions on the classical Coulomb trajectory; around this angle, the semiclassical description is in excellent agreement with the quantal description. Deviations from the mean-field electron screening are weak and manifest themselves only in backward scattering. Semiclassical total cross sections are practically equal to the Coulomb-Born predictions. This near equality is explained within the WKB approximation. The practical equivalence between the semiclassical, WKB, and Coulomb-Born approximations applies also for other multipoles in a wide range of energy, energy transfer, and ionic charge.

PACS number(s): 34.80.Kw

I. INTRODUCTION

With the recent availability of intense beams, it has become feasible to measure total and differential cross sections for excitation of multiply charged ions by electron impact. Apart from measurements on singly charged ions, absolute total excitation cross sections for multiply charged ions have been limited to a few systems: (Hg^{2+}, Al^{2+}, C^{3+}, Si^{3+}, N^{4+}) [1], Ba^{46+} [2], and Ti^{20+} [3]. To our knowledge, differential cross sections have been measured so far only for ${}^2S_{\frac{1}{2}} \rightarrow {}^2S_{\frac{1}{2}}$, ${}^2S_{\frac{1}{2}} \rightarrow {}^2P_{\frac{1}{2},\frac{3}{2}}$, and for ${}^2S_{\frac{1}{2}} \rightarrow {}^2D_{\frac{3}{2},\frac{5}{2}}$ transitions in the singly charged alkali-metal-like ions Mg^+, Zn^+, and Cd^+ [4] and for the ${}^2S_{\frac{1}{2}} \rightarrow {}^2P_{\frac{1}{2},\frac{3}{2}}$ transition in the multiply charged sodiumlike Ar^{7+} [5]. It is worth noting that, in all these differential-cross-section experiments, measurements were restricted to forward scattering, and that the incident energy was a few times the transition energy. The theoretical predictions of these differential excitation cross sections have so far been limited to the singly charged ions and have been worked out within either the close-coupling approximation (CCA) [6–8] or the distorted-wave Born approximation (DWBA) [9]. The validity of the DWBA for total and differential excitation cross sections in the case of multiply charged ions has been thoroughly investigated by Pindzola and co-workers [10, 11] who made comparisons with CCA predictions. Relativistic effects on total excitation cross sections, also investigated in the DWBA, have been found to be quite sizable for highly charged ions [12].

In the present paper, we calculate the differential cross section for the excitation of the lowest dipole transition in alkali-metal-like ions by electron impact. Consistent with the experiment of Huber *et al.* [5], we consider the excitation of Ar^{7+} at a 100 eV incident energy, that is, about six times the threshold energy. Other alkali-metal-like ions at the same relative energy are also considered. The calculations are first carried out in the generalized Born approximation with continuum wave functions being given by either a pure Coulomb potential as in the Coulomb-Born approximation (CBA) or by a more realistic atomic potential as in the DWBA. The CBA serves as a reference for a semiclassical calculation. In this semiclassical approximation it is assumed that the electron projectile follows a classical Coulomb trajectory and the excitation process is treated in the first order of time-dependent perturbation theory. This is similar to the semiclassical theory of the Coulomb excitation of atomic nuclei [13].

II. THEORY

A. Distorted-wave Born approximation

The excitation of neutral atoms by electron impact has been investigated thoroughly with elaborate models such as the close-coupling approximation. The excitation of positive ions usually demands less theoretical sophistication simply because of the dominant contribution of the long-range potential. A rather simple and powerful method is given by the DWBA where the coupling between various excitation channels is neglected. In this first-order perturbation theory approach, the initial state is made of the product of the projectile wave function in some model potential and the target wave function obtained to some desired approximation. The final state is described in the same manner. For the sake of clarity and in keeping with the experiment [5], we consider here the lowest excitations of alkali-metal-like ions. The excitation goes through the valence electron from the n_a s ground state to a n_b l_b excited state. Using atomic units $\hbar = m = e = 4\pi\epsilon_0 = 1$, the excitation cross section for the transition is expressed as

$$\frac{d\sigma}{d\Omega} = \frac{1}{4\pi^2}\frac{p_f}{p_i} \times \sum_{m_b}\left|\langle\Psi_f(\mathbf{r})\Phi_b(\mathbf{r}')\left|\frac{1}{|\mathbf{r}-\mathbf{r}'|}\right|\Phi_a(\mathbf{r}')\Psi_i(\mathbf{r})\rangle\right|^2 \quad (1)$$

where the coordinates $\mathbf{r}$ and $\mathbf{r}'$ are for the scattering electron and the valence electron, respectively. The initial and final electron wave functions Ψ_i and Ψ_f have momenta p_i and p_f, respectively. Assuming that the closed shell is a spectator, the target ground state is described by the valence electron wave function Φ_a while the excited valence state is described by Φ_b. Let us introduce the transition potential defined as

$$V_T(ab;\mathbf{r}) = \langle\Phi_b(\mathbf{r}')\left|\frac{1}{|\mathbf{r}-\mathbf{r}'|}\right|\Phi_a(\mathbf{r}')\rangle. \quad (2)$$

The transition potential contains the structural information of the target. In the present work, it has been calculated with Hartree-Fock wave functions. Correlation effects such as the core polarization may be included; however, they do not contribute significantly [14] in multiply charged ions and will not be considered in the present work. For very highly charged ions it would be appropriate to use relativistic self-consistent wave functions [12]. Results on relativistic effects on differential cross sections will be discussed elsewhere [14]. As usual, the Coulomb interaction is expanded as

$$\frac{1}{|\mathbf{r}-\mathbf{r}'|} = \sum_{\lambda,m}\frac{4\pi}{2\lambda+1}\frac{r_<^\lambda}{r_>^{\lambda+1}}Y^*_{\lambda m}(\hat{\mathbf{r}})Y_{\lambda m}(\hat{\mathbf{r}'}) \quad (3)$$

and the bound state wave function as

$$\Phi(\mathbf{r}') = \frac{P_{nl}(r')}{r'}Y_{lm}(\hat{\mathbf{r}'})\chi_{m_s} \quad (4)$$

leading to

$$V_T(ab;\mathbf{r}) = \frac{\sqrt{4\pi}}{2l_b+1}\mathcal{V}_{l_b}(ab;r)Y_{l_b m_b}(\hat{\mathbf{r}}). \quad (5)$$

The multipole component $\mathcal{V}_\lambda$ is given by

$$\mathcal{V}_\lambda = \frac{1}{r_>^{\lambda+1}}\int_0^r P_b(r')r'^\lambda P_a(r')dr' + r^\lambda\int_r^\infty P_b(r')\frac{1}{r'^{\lambda+1}}P_a(r')dr'. \quad (6)$$

This allows us to write the differential cross section as

$$\frac{d\sigma}{d\Omega} = \frac{1}{4\pi^2}\frac{p_f}{p_i}\sum_{m_b}|\langle\Psi_f|V_T|\Psi_i\rangle|^2, \quad (7)$$

where the scattering states are eigenstates of the distorting potential. Generally the outgoing (initial) and incoming (final) states can be expanded as

$$\Psi_i(\mathbf{r}) = \sum_{l_i,m_i}4\pi(-)^{m_i}i^{l_i}e^{i\delta_{l_i}}Y_{l_i-m_i}(\hat{\mathbf{p}}_\mathbf{i}) \times Y_{l_i m_i}(\hat{\mathbf{r}})\frac{1}{p_i r}F_{l_i}(p_i r), \quad (8)$$

$$\Psi_f(\mathbf{r}) = \sum_{l_f,m_f}4\pi(-)^{m_f}i^{l_f}e^{-i\delta_{l_f}}Y_{l_f-m_f}(\hat{\mathbf{p}}_\mathbf{f}) \times Y_{l_f m_f}(\hat{\mathbf{r}})\frac{1}{p_f r}F_{l_f}(p_f r). \quad (9)$$

In the CBA the distorting potential is simply $-Z/r$, Z being the ionic charge, leading to the well-known analytical expressions for the Coulomb phase shift and radial function:

$$\delta_l = \arg\Gamma(l+1+i\eta), \quad (10)$$

$$F_l(pr) = \frac{|\Gamma(l+1+i\eta)|}{2(2l+1)!}e^{-\frac{1}{2}\eta\pi}(2pr)^{l+1} \times e^{-ipr}M(l+1-i\eta,2l+2,+2ipr) \quad (11)$$

with the asymptotic behavior:

$$F_l(pr) \sim \sin\left(pr - l\frac{\pi}{2} - \eta\ln(2pr) + \delta_l\right) \quad (12)$$

with η being the Sommerfeld parameter $\eta = -\frac{Z}{p}$. In the DWBA, one simply adds to the Coulomb potential the screening potential due to the electrons. The radial continuum wave function is calculated in the chosen distorting potential and the total phase shift is obtained by properly adjusting the continuum radial wave function to the Coulomb asymptotic behavior of Eq. (12). This total phase shift is thus the sum of the above Coulomb phase shift and a short range contribution. By assigning the initial momentum p_i to be along the z axis, the differential cross section can be written as

$$\frac{d\sigma}{d\Omega} = \frac{16\pi}{p_i^3 p_f}\sum_{m_b}\left|\sum_{l_i,l_f}i^{(l_i-l_f)}e^{i[\delta_{l_i}+\delta_{l_f}]} \times Y_{l_f-m_b}(\hat{\mathbf{p}}_\mathbf{f})\mathcal{A}^{l_b}_{l_i l_f}\mathcal{R}^{l_b}_{l_i l_f}\right|^2, \quad (13)$$

$$\mathcal{A}^{l_b}_{l_i l_f} = (2l_i+1)\sqrt{\frac{2l_f+1}{2l_b+1}}\begin{pmatrix} l_f & l_b & l_i \\ 0 & 0 & 0\end{pmatrix}\begin{pmatrix} l_f & l_b & l_i \\ -m_b & m_b & 0\end{pmatrix}, \quad (14)$$

$$\mathcal{R}^{l_b}_{l_i l_f} = \int_0^\infty F_{l_f}(p_f r)\mathcal{V}_{l_b}(ab;r)F_{l_i}(p_i r)dr. \quad (15)$$

The total cross section is in turn expressed as

$$\sigma_{\text{tot}} = \frac{16\pi}{p_i^3 p_f}\frac{1}{(2l_b+1)}\sum_{l_i,l_f}(2l_i+1)(2l_f+1)\begin{pmatrix} l_f & l_b & l_i \\ 0 & 0 & 0\end{pmatrix}^2 \times\left[\mathcal{R}^{l_b}_{l_i l_f}\right]^2. \quad (16)$$

The expression for the DWBA amplitude given in Eq. (1) does not account for the indistinguishability between the projectile electron and the electron in the target. In actual calculations one has to include the exchange effects by multiplying the Coulomb potential operator by $(1-P)$ where P is the exchange operator. We shall show

in the next section that these exchange contributions are negligible at the energies of interest for the present problem.

B. Semiclassical approximation

The present semiclassical model for the excitation of multiply charged ions by electron impact is very similar to that of the Coulomb excitation of nuclei by positively charged heavy ions as worked out by Alder *et al.* [13]. The projectile is assumed to follow a classical Coulomb trajectory and the excitation of the target is described in the framework of first-order time dependent theory. This perturbation is assumed not to affect the projectile trajectory. Thus the differential excitation cross section in the semiclassical approximation (SCA) is written as

$$\frac{d\sigma}{d\Omega} = P_{ab}\left[\frac{d\sigma}{d\Omega}\right]_R \tag{17}$$

with the Rutherford cross section:

$$\left[\frac{d\sigma}{d\Omega}\right]_R = \frac{1}{4}a_c^2\frac{1}{\sin^4(\theta/2)} \tag{18}$$

and $a_c = -Z/2E$ being the characteristic length of the scattering problem. The probability P_{ab} of excitation from the ground state a to the excited state b is given by

$$P_{ab} = \sum_{m_b} |b_{ab}|^2 \tag{19}$$

with

$$b_{ab} = \frac{1}{i}\int_{-\infty}^{+\infty} \langle \Phi_b | \frac{1}{|\mathbf{r}(t) - \mathbf{r}'|} | \Phi_a \rangle e^{i\omega t} dt, \tag{20}$$

$$b_{ab} = \frac{\sqrt{4\pi}}{2l_b+1}\frac{1}{i}\int_{-\infty}^{+\infty} \mathcal{V}_{l_b}(ab; r(t)) Y_{l_b m_b}(\hat{\mathbf{r}}(t)) e^{i\omega t} dt. \tag{21}$$

In order to perform the time integration along the Rutherford trajectory it is convenient to define a new inertial frame as described in textbooks [15]. In this frame (see Fig. 1) the Cartesian coordinates of the projectile are parametrized as

$$\begin{aligned} x &= a_c(\cosh(\nu) + \epsilon), \\ y &= a_c\sqrt{\epsilon^2 - 1}\sinh(\nu), \\ z &= 0, \\ r &= a_c(\epsilon\cosh(\nu) + 1), \\ t &= \tfrac{a_c}{p_i}(\epsilon\sinh(\nu) + \nu), \end{aligned} \tag{22}$$

where the eccentricity is defined as $\epsilon = -\frac{1}{\sin(\theta/2)}$. In order to symmetrize the classical description and to fulfill the requirement of detailed balance, that is, the ratio of the cross sections for transitions $a \to b$ and $b \to a$ is equal to the ratio p_f/p_i, we define a mean trajectory by introducing an effective length $\tilde{a_c}$ as

$$\tilde{a_c} = -\frac{Z}{p_i p_f}. \tag{23}$$

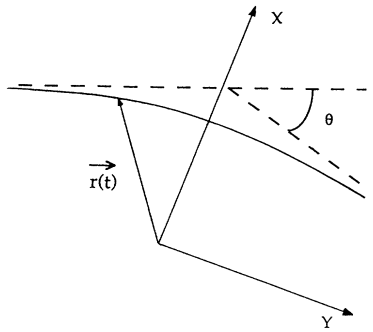

FIG. 1. Classical picture of the electron orbit in the Coulomb field of the positive ion. The position of the electron and the deflection angle are denoted by $\mathbf{r}(t)$ and θ, respectively.

After some algebraic manipulations one obtains

$$b_{ab} = \frac{1}{i}\frac{\sqrt{4\pi}}{2l_b+1}Y_{l_b m_b}\left(\frac{\pi}{2}, 0\right)\frac{\tilde{a_c}}{p_i}\mathcal{I}_{ab}^{m_b}(\epsilon, \xi) \tag{24}$$

with

$$\begin{aligned} \mathcal{I}_{ab}^{m_b}(\epsilon, \xi) = \int_{-\infty}^{+\infty} & e^{i\xi(\epsilon\sinh(\nu)+\nu)} \\ & \times \frac{[\cosh(\nu) + \epsilon + i\sqrt{\epsilon^2-1}\sinh(\nu)]^{m_b}}{[\epsilon\cosh(\nu)+1]^{m_b-1}} \\ & \times \mathcal{V}_{l_b}(ab; r) d\nu, \end{aligned} \tag{25}$$

where the dimensionless quantity ξ is defined as

$$\xi = \eta_f - \eta_i. \tag{26}$$

The semiclassical differential cross section is finally expressed as

$$\frac{d\sigma}{d\Omega} = \frac{1}{4}\tilde{a_c}^2\frac{1}{\sin^4(\theta/2)}\sum_{m_b}|b_{ab}|^2 \tag{27}$$

and the total cross section as

$$\sigma_{\text{tot}} = -2\pi\tilde{a_c}^2\int_{-\infty}^{-1} d\epsilon\,\epsilon\sum_{m_b}|b_{ab}|^2. \tag{28}$$

C. WKB approximation

We shall now recall the link between the quantal description and the semiclassical one as demonstrated in Ref. [13] for the nuclear case. The WKB approximation of the radial wave function of Eq. (11) is given by

$$F_l(pr) = \left(\frac{f(r)}{p^2}\right)^{-\frac{1}{4}}\sin\varphi, \tag{29}$$

where

$$\varphi = \frac{\pi}{4} + \int_{r_0}^{r} dr f(r)^{\frac{1}{2}} \tag{30}$$

and

$$f(r) = p^2 - 2\frac{p\eta}{r} - \frac{l(l+1)}{r^2}. \tag{31}$$

The turning point r_0 is the solution to the equation $f(r_0) = 0$. Note that, in the present case of an attractive Coulomb potential, the classically forbidden region where $r < r_0$ is encountered only for large l values, thus supporting the WKB approximation. Substituting the WKB wave function Eq. (29) into Eq. (15) one finds

$$\mathcal{R}^{l_b}_{l_i l_f} = \frac{1}{2}\int_0^\infty \frac{[f_i(r)f_f(r)]^{-\frac{1}{4}}}{(p_i p_f)^{-\frac{1}{2}}} \times \{\cos(\varphi_i - \varphi_f) - \cos(\varphi_i + \varphi_f)\} \times \mathcal{V}_{l_b}(ab;r)dr. \tag{32}$$

The second cosine function, of which the argument is the sum of the phases, oscillates rapidly and can therefore be safely neglected. After a few manipulations, the difference $\varphi_i - \varphi_f$ can be approximated as

$$\varphi_i - \varphi_f = \xi(\epsilon\sinh\nu + \nu) + \mu\arccos\left[\frac{\epsilon + \cosh\nu}{\epsilon\cosh\nu + 1}\right], \tag{33}$$

where we have made the following substitutions:

$$\begin{aligned} &\mu = l_i - l_f, \\ &\tilde{l} = \tfrac{l_i + l_f}{2}, \\ &\tilde{p} = \sqrt{p_i p_f}, \\ &\tilde{\eta} = -\tfrac{Z}{\tilde{p}}, \\ &\tilde{p}r = [\tilde{\eta}^2 + \tilde{l}(\tilde{l}+1)]^{\frac{1}{2}}\cosh\nu + \tilde{\eta}, \\ &\tilde{\epsilon} = \tfrac{[\tilde{\eta}^2 + \tilde{l}(\tilde{l}+1)]^{\frac{1}{2}}}{\tilde{\eta}}. \end{aligned} \tag{34}$$

The resulting WKB approximation for the matrix element can then be written as

$$\mathcal{R}^{l_b}_{l_i l_f} = \frac{\tilde{\eta}}{4\tilde{p}}\int_{-\infty}^{+\infty} e^{i\xi(\epsilon\sinh(\nu)+\nu)} \times \frac{[\cosh(\nu) + \epsilon + i\sqrt{\epsilon^2 - 1}\sinh(\nu)]^{\mu}}{[\epsilon\cosh(\nu) + 1]^{\mu-1}} \times \mathcal{V}_{l_b}(ab;r)d\nu, \tag{35}$$

where the integral is just identical, with $\mu = m_b$, to the integral Eq. (25) derived in the semiclassical approximation. In order to work out the total cross section, we replace the partial wave summation of Eq. (16) by an integral over the angle θ defined along the Rutherford trajectory as

$$\tilde{l} = -\tilde{\eta}\cot(\theta/2) \tag{36}$$

and we use the approximation

$$(2l_i+1)(2l_f+1)\begin{pmatrix} l_f & l_b & l_i \\ 0 & 0 & 0 \end{pmatrix}^2 \simeq (2\tilde{l}+1)\frac{4\pi}{2l_b+1}\left[Y_{l_b\mu}\left(\frac{\pi}{2},0\right)\right]^2. \tag{37}$$

One then finds that the total WKB cross section is just equal to the semiclassical cross section given by (28).

III. RESULTS AND DISCUSSIONS

In the following we present cross sections calculated for various multipole excitations of alkali-metal-like ions obtained in the DWBA, the CBA, and the SCA.

A. Dipole excitations

For multiply charged ions, the dipole transition potential defined in Eq. (2) is dominated by the $1/r^2$ part that extends well outside the electron density and whose strength is actually given by the ns-np dipole strength. As an illustration, the radial dependence of this potential is shown in Fig. 2. We therefore do not expect the angular distribution to be very sensitive to the detailed electronic structure but rather to exhibit features that are characteristic of the long-range Coulomb scattering problem.

Differential cross sections for the first ns-np dipole excitation of lithiumlike ions (Be^+, Ne^{7+}, Ni^{25+}), sodiumlike ions (Mg^+, Ar^{7+}, Kr^{25+}), potassiumlike ions (Ca^+, Fe^{7+}, Ru^{25+}), and rubidiumlike ions (Sr^+, Ru^{7+}, Sm^{25+}) have all been calculated at the same ratio, x, of incident energy over transition energy equal to 5.76. This value of x corresponds to the excitation of the $3s$-$3p$ transition in Ar^{7+} by a 100-eV electron for which experimental data are available [5]. In Figs. 3(a)–3(d) we compare the predictions of the DWBA and the CBA. The potential that is used in the DWBA is the Hartree-Fock potential obtained by solving the self-consistent equations for the target electrons. The entrance channel and exit channel potentials are obtained with the target in its ground state and excited state, respectively. In all cases the exchange contributions which involve only the valence electron and the projectile are taken into account. For the least favorable case of singly charged ions these contributions are small and significant only at backward angles as demonstrated in Fig. 4. As previously reported [5], an excellent agreement with the experimental data on Ar^{7+} is found. No other experimental data are available except for Mg^+,

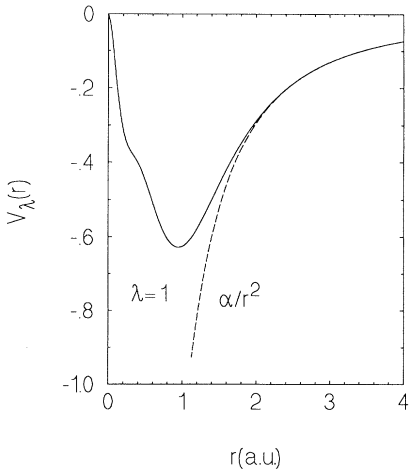

FIG. 2. Radial part of the dipole transition potential for the $3s$-$3p$ transition of Ar^{7+}.

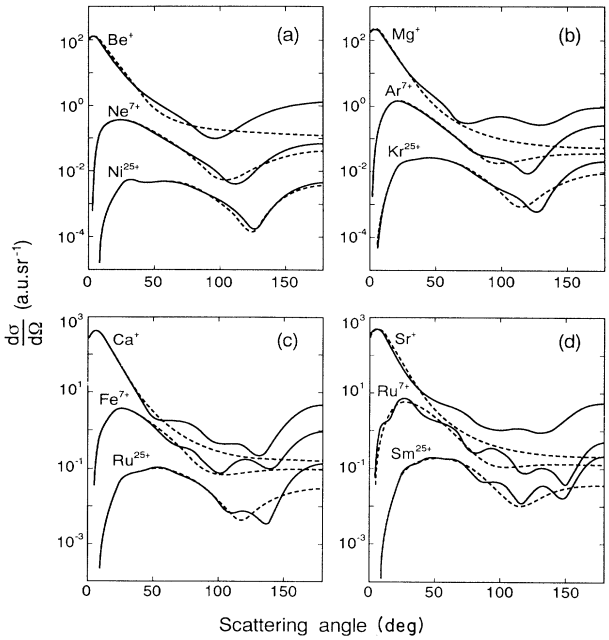

FIG. 3. Calculated differential cross sections for excitation of the ns-np transition of alkali-metal-like ions by electron impact at an energy equal to 5.76 times the transition energy. The solid curve refers to the DWBA and the dashed curve to the CBA. (a), (b), (c), and (d) are for Li-like ($2s$-$2p$), Na-like ($3s$-$3p$), K-like ($4s$-$4p$), and Rb-like ($5s$-$5p$) ions, respectively.

and these have unfortunately been normalized to theory [4].

The DWBA and CBA angular distributions exhibit a common gross feature. The angle of maximum cross section moves from near zero degree for singly charged ions up to about 50° for $Z = 25$. Note that this shift was already emphasized by Mitroy [16, 17] in a CBA calculation on Mg^+ at 20- and 50-eV incident energy and Be^+ over a broad energy range. This Coulomb shift of the maximum cross section angle is also found in the SCA where predictions are compared to those of the CBA in Figs. 5(a)–5(d). This leads to a classical interpretation in terms of a most probable projectile trajectory for the excitation at stake. In order to transfer efficiently the excitation energy ΔE from the relative motion to the target, the collision time τ_c should be lower than $1/\Delta E$. This will in turn preclude trajectories characterized by an impact parameter too large to fulfill the collision time criteria. For a Coulomb trajectory the collision time is related to the distance of closest approach, $r_{\min}$, by

$$\tau_c = \frac{r_{\min}}{v} = \frac{a_c(1+\epsilon)}{v}. \tag{38}$$

Using the relation $\epsilon = -\frac{1}{\sin(\theta/2)}$ for the mean trajectory, we obtain a critical angle $\theta_{\rm cr}$, below which there is no transition, defined as

$$\theta_{\rm cr} = 2\arcsin\left(\frac{\xi}{1+\xi}\right) \tag{39}$$

with ξ being the adiabaticity parameter of Eq. (26) which in the present case of a fixed x ratio can be written as

$$\xi \simeq \frac{1}{(2x)^{\frac{3}{2}}}\frac{Z}{\sqrt{\Delta E}}. \tag{40}$$

It is justified to take this value of $\theta_{\rm cr}$ as the most probable

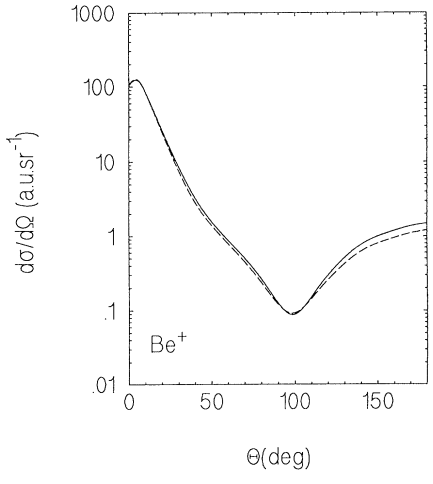

FIG. 4. DWBA differential cross sections for excitation of the $2s$-$2p$ transition of Be^+ by electron impact at an energy equal to 5.76 times the transition energy. Exchange contributions are omitted in the solid curve and included in the dashed curve.

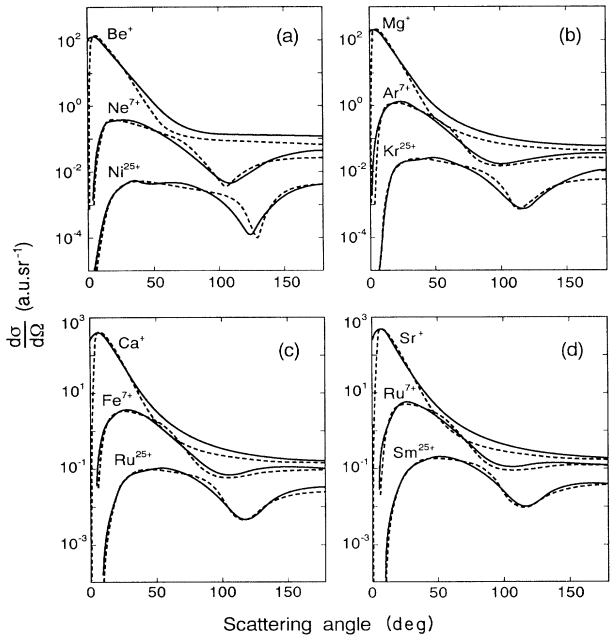

FIG. 5. Calculated differential cross sections for excitation of the ns-np transition of alkali-metal-like ions by electron impact at an energy equal to 5.76 times the transition energy. The solid curve refers to the CBA and the dashed curve to the SCA. (a), (b), (c), and (d) are for Li-like ($2s$-$2p$), Na-like ($3s$-$3p$), K-like ($4s$-$4p$), and Rb-like ($5s$-$5p$) ions, respectively.

one since the Rutherford cross section in the forward direction falls very rapidly with angle. By noting that along an isoelectronic sequence, the *ns-np* transition energy scales linearly as $(Z+1)$, we expect the parameter ξ to vary approximatively as $\sqrt{Z}$. The subsequent expected variation of θ_{cr} with the ionic charge is in fair agreement with the theoretical calculations. It is worth noting that the ratio $(\frac{\xi}{1+\xi})$ depends almost only on the ionic charge so that angular distributions for isoionic systems should peak at about the same angle. This behavior is well confirmed by our calculations and can be seen by comparing Figs. 3(a)–3(d). For dipole transitions in highly charged ions, with a change of the principal quantum number, the parameter ξ is independent of the charge and so should approximately be the angular distribution. This is well verified by DWBA calculations on He-like ions [18].

It is worth emphasizing the excellent agreement of the SCA and the CBA in their respective predictions of differential cross sections, as was expected from the discussion of the preceding section. The agreement is observed over a wide range of the relative incident energy, x, as shown in Figs. 6(a) and 6(b) for $x=2$ and $x=10$. The lower value of $x=2$ is only of theoretical interest since the CBA itself is at its limit of validity. The SCA can, however, be extended to any distorting potential requiring a numerical integration over a classical trajectory in this new potential.

Along a given isoelectronic sequence the deviations of the DWBA predictions from the CBA ones decrease with increasing Z but become signifiant only at angles well above the most probable angle. As the electronic structure gets more complex, the backward inelastic scattering is characterized by quantal oscillations due to the interference between the long-range Coulomb phase and the short-range electron screening phase. However, these screening corrections do not affect sensitively the total cross section as shown in Table I.

As can be seen from Table I, the total cross section obtained in the SCA never differs by more than 0.5% from the one calculated in the Coulomb-Born approximation without exchange. This excellent agreement has been checked over a broad range of x values [14]. Moreover, this SCA total cross section is an excellent approximation within a few percent of the DWBA prediction, discrepancies being significant only for singly charged ions.

Being aware of the experimental difficulties in measuring precisely absolute excitation cross sections of multiply charged ions by electron impact, we show in Figs. 7(a)–7(d) the ratio of the *ns-np* differential cross section over the elastic cross section. The latter has been derived from a calculation of the scattering phase shifts in the Hartree-Fock approximation. The short-range phase shift brings deviations from the pure Rutherford elastic cross section only at angles higher than the most probable inelastic angle. We believe that the Hartree-Fock approximation is excellent and have checked that polarization effects are negligible in the present case, which is characterized by an incoming electron energy equal to 5.76 times the excitation threshold. In all cases the ratio increases abruptly from 0° to a first maximum at an angle located above the most probable excitation angle of Figs. 3(a)–3(d). Then the ratio goes through a minimum and increases again at backward angles. Such a behavior will soon be checked experimentally on Ar^{7+} [19].

B. Other multipole excitations

For excitations of multipolarity L larger than 1 the situation is rather similar to the dipole case. The asymptotic transition potential of Eq. (6) is characterized by a $1/r^{L+1}$ tail. CBA and SCA calculations of total cross sections for the first quadrupole transition *ns-nd* in Ar^{7+} are in full agreement with each other as shown in Table

TABLE I. Calculated total cross sections (atomic units) for the first dipole excitation (*ns-np*) of lithiumlike ions, sodiumlike ions, potassiumlike ions, and rubidiumlike ions. The relative incident energy is equal to 5.76 times the transition energy calculated in the Hartree-Fock approximation. Various approximations are given: distorted-wave Born approximation with exchange (DWBA) and without exchange (DWBA*), Coulomb-Born approximation with exchange (CBA) and without exchange (CBA*), semiclassical approximation with Coulomb trajectories (SCA).

Ion	DWBA	DWBA*	CBA	CBA*	SCA
Be^{+}	38.40	40.64	39.42	41.51	41.81
Ne^{7+}	0.949	0.987	0.944	0.978	0.986
Ni^{25+}	0.0318	0.0327	0.0313	0.0321	0.0324
Mg^{+}	53.92	56.92	53.27	56.22	56.36
Ar^{7+}	2.571	2.666	2.501	2.569	2.575
Kr^{25+}	0.126	0.130	0.123	0.125	0.125
Ca^{+}	130.9	137.8	129.9	136.3	136.5
Fe^{7+}	8.446	8.694	8.082	8.294	8.308
Ru^{25+}	0.518	0.529	0.496	0.503	0.504
Sr^{+}	158.5	165.5	162.7	170.3	170.5
Ru^{7+}	12.59	12.94	12.27	12.55	12.56
Sm^{25+}	0.984	1.001	0.927	0.941	0.942

II. For monopole transitions, the asymptotic transition potential has only one term which decays exponentially. This transition potential is thus of much shorter range than other multipoles and acts only inside the ion. Concerning the total excitation cross sections the arguments developed in Sec. II C are fully valid (only a few partial waves contribute), and as expected and shown in Table II the CBA and SCA predictions just agree within less than 0.3%. However, the quantal and semiclassical angular distributions differ considerably at forward angles as seen in Fig. 8. The CBA predicts two maxima, one being at 0° whereas the SCA yields only one which is close to the second maximum of the former approximation and well explained by the classical argument discussed above.

IV. CONCLUSION

In the paragraphs above, we have shown that total cross sections for dipole excitation of alkali-metal-like multiply charged ions by electron impact at energies well above threshold are given to a very good accuracy by a semiclassical model in which it is assumed that the electron projectile moves on a classical Coulomb trajectory. Such an approach could be extended to other multicharged ions since the structure information is entirely contained in the transition potential. Once this poten-

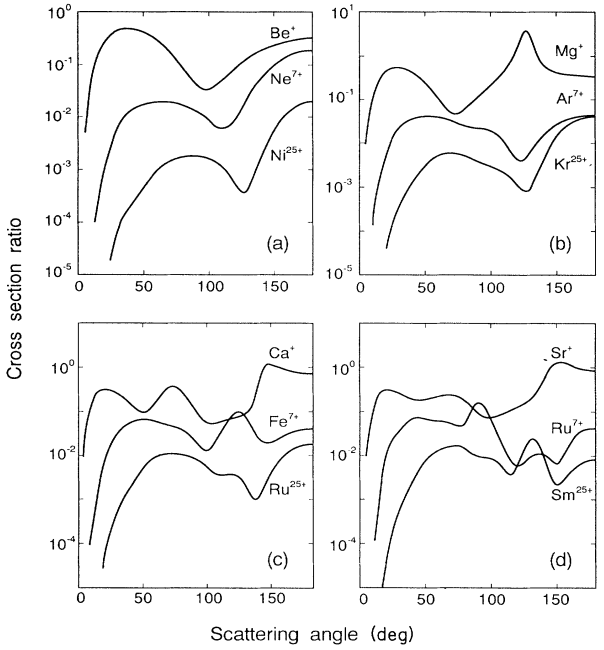

FIG. 7. Ratio of DWBA differential cross section for excitation of the *ns-np* transition of alkali-metal-like ions by electron impact over elastic cross section. The electron energy is equal to 5.76 times the transition energy. (a), (b), (c), and (d) are for Li-like (2*s*-2*p*), Na-like (3*s*-3*p*), K-like (4*s*-4*p*), and Rb-like (5*s*-5*p*) ions, respectively.

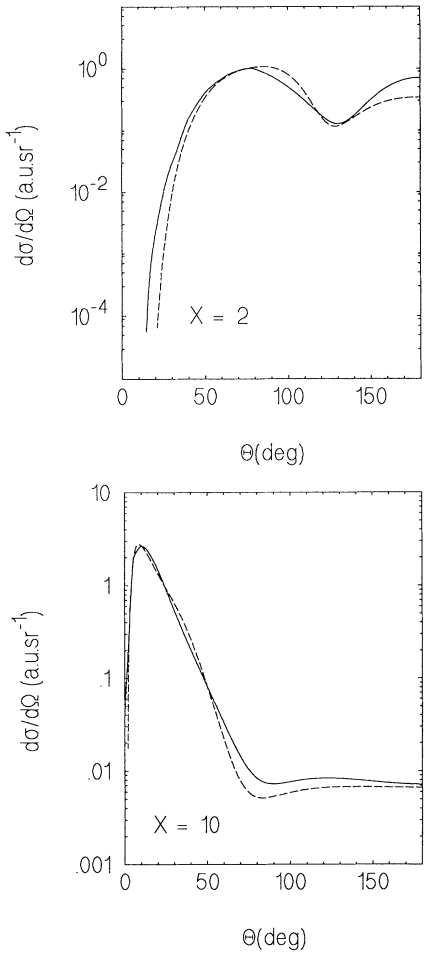

FIG. 6. CBA (solid line) and SCA (dashed line) calculations of the differential cross section for excitation of the 3*s*-3*p* transition of Ar^{7+} by electron impact at an energy equal to 2 times the transition energy (a) and 10 times the transition energy (b).

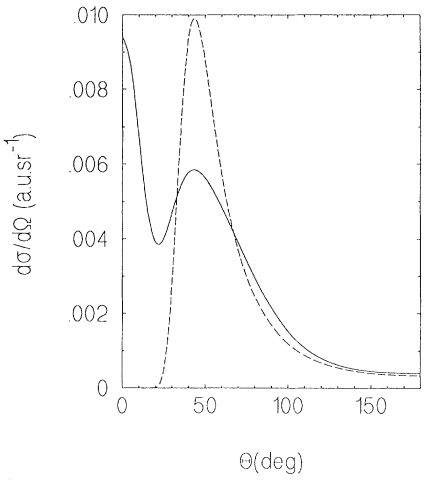

FIG. 8. CBA (solid line) and SCA (dashed line) calculations of the differential cross section for excitation of the 3*s*-4*s* transition of Ar^{7+} by electron impact at an energy equal to 3 times the transition energy.

TABLE II. Calculated total cross sections (atomic units) for the ($3s$-$4s$) monopole and the ($3s$-$3d$) quadrupole excitations of Ar^{7+}. The relative incident energy is equal to 5.76 times the transition energy calculated in the Hartree-Fock approximation. Various approximations are given: Coulomb-Born approximation without exchange (CBA*) and semiclassical approximation with Coulomb trajectories (SCA).

Excitation	CBA*	SCA
$3s$-$4s$	0.0177	0.0177
$3s$-$3d$	0.114	0.114

tial has been calculated within some atomic model—with configuration interactions for instance—it merely remains to perform the time integration along the classical trajectory, thus avoiding the lengthy partial-wave expansion that the DWBA requires and that, in this Coulomb context, extends to large l values. This is particularly useful for differential cross sections which require one to go to very high angular momenta indeed. We showed that the semiclassical and Coulomb-Born approximations give very similar angular distributions. We showed that the CBA is valid up to a large angle and that electronic screening plays a role only at backward angles. The strong Coulomb field which affects the projectile is responsible for a strong shift of the dipole angular distribution that peaks at an angle roughly estimated by matching the collision time and the inverse-transition frequency. It was also shown that this semiclassical approximation is valid for total cross sections of other multipole excitations. This is reminiscent of the equivalence between the Born approximation and the semiclassical approximation with straight-line trajectories. Note, however, that for a monopole transition, the angular distributions cannot be properly described within the semiclassical approximation.

ACKNOWLEDGMENTS

The authors would like to thank S. Blundell, P. Defrance, J. P. Desclaux, B. A. Huber, W. Johnson, and C. Ristori for stimulating discussions.

[1] E.K. Waahlin, J.S. Thompson, G.H. Dunn, R.A. Phaneuf, D.C. Gregory, and A.C.H. Smith, Phys. Rev. Lett. **66**, 157 (1991), and references therein.
[2] R.E. Marrs, M.A. Levine, D.A. Knapp, and J.R. Henderson, Phys. Rev. Lett. **60**, 1715 (1988).
[3] S. Chantrenne, P. Beiersdorfer, R. Cauble, and M.B. Schneider, Phys. Rev. Lett. **69**, 265 (1992).
[4] I.D. Williams, A. Chutjian, and R.J. Mawhorter, J. Phys. B **19**, 2189 (1986).
[5] B.A. Huber, Ch. Ristori, P.A. Hervieux, M. Maurel, C. Guet, and H.J. Andrä, Phys. Rev. Lett. **67**, 1407 (1991).
[6] A.Z. Msezane and R.J.W. Henry, Phys. Rev. A **25**, 692 (1982).
[7] A. Chutjian, A.Z. Msezane, and R.J.W. Henry, Phys. Rev. Lett. **50**, 1357 (1983).
[8] I.D. Williams, A. Chutjian, A.Z. Msezane, and R.J.W. Henry, Astrophys. J. **299**, 1063 (1985).
[9] A.W. Pangantiwar and R. Srivastava, J. Phys. B **21**, L219 (1988).
[10] M.S. Pindzola, D.C. Griffin, and C. Bottcher, Phys. Rev. A **39**, 2385 (1989).
[11] M.S. Pindzola, D.C. Griffin, and N. R. Badnell (unpublished).
[12] Y.K. Kim and J.P. Desclaux, Phys. Scr. **36**, 796 (1987).
[13] K. Alder, A. Bohr, T. Huus, B. Mottelson, and A. Winther, Rev. Mod. Phys. **28**, 432 (1956).
[14] P.A. Hervieux, thesis, Université Joseph Fourier, Grenoble, France, 1992.
[15] L. Landau and E. Lifchitz, *Mécanique* (MIR, Moscow, 1969).
[16] J. Mitroy, Phys. Rev. A **37**, 649 (1988).
[17] J. Mitroy, J. Phys. B **21**, L25 (1988).
[18] R. Srivastava, Y. Itikawa, and K. Sakimoto, Phys. Rev. A **43**, 4736 (1991).
[19] B.A. Huber and C. Ristori (private communication).